

Using MPC as Master Controller for Integrated Gasification Combined Cycle Processes

F. Rusconi*, A. Bemporad[#]♦, M. Morari♦, M. Rovaglio^{*}▲

** Dipartimento di Chimica, Materiali ed Ingegneria Chimica "G. Natta"
Politecnico di Milano, P.zza Leonardo da Vinci 32, 20133 Milano, Italy*

*[#]Dipartimento di Ingegneria dell'Informazione, Università di Siena,
Via Roma 56, 53100 Siena, Italy*

*♦ Automatic Control Laboratory, ETH Zentrum, ETL I 29
CH8092 Zurich, Switzerland*

▲ corresponding author, e-mail: maurizio.rovaglio@polimi.it

The aim of this work is the design of a master controller for an IGCC (Integrated Gasification Combine Cycle) plant, based on an MPC (Model Predictive Control) approach, which is able to coordinate the main process variables interacting with the basic structure of standard controllers at the unit level. Generally, a master controller is obtained by conventional loops based on a "pressure driven" configuration. In the following, the MPC library for MATLAB (by Bemporad, Morari and Ricker, 2000) has been applied to a detailed IGCC plant simulation tool in order to understand the performance of a reliable multivariable linear MPC when adopted for such a nonlinear complex process with crucial targets. A detailed first principle model has been used as a "real plant" when performing the step tests for the identification of the simplified linear model and when checking the reliability of the control tool. Moreover, the effectiveness of the designed controller has been proved through the comparison between the linear MPC approach and an ideal solution ("direct" approach) obtained by the direct inversion of the DAE model, where perfect setpoint tracking is imposed by additional constraint equations and using the corresponding manipulated variables as closing variables. Moreover the performance of the derived MPC controller, when compared with a more conventional control configuration, shows a significant reduction of the overshoots and settling time when the plant is subject to load variations. The paper clearly shows how the MPC approach for a master controller is reliable, easy to design and of real value for practical purposes.

Introduction

Refinery plants often use a thermal conversion (like visbreaking or thermal cracking) in order to produce GPL and gasoline from heavy residuals. The remainder (15% of the original crude feed) is a product called *Tar* or, more in general, *Char*. The features of such a product are: high viscosity, high sulfur content but also high total heating value corresponding to the heat released when the residual is totally burned (around 9300 kcal/kg). Therefore, due the recent deregulation in terms of power production and since in the refinery many of the necessary technologies and utilities are already present, it is a common trend to realize Integrated Gasification Combined Cycle processes where the aforementioned residuals are used as the main feed for energy production (Parkinson and Fouhy, 1996). The process consists of the following main steps: gasification of the fuel (*char*) producing a syngas rich in CO and H₂, gas purification with sulfur removal and a Combined Cycle Unit (CCU) with gas/steam turbines and boiler section for total heat recovery. This solution leads to a significant production of electrical energy for the network plus steam and hydrogen for the refinery.

For their utility nature, IGCC plants are subject to fast variations of external power and steam demands and the control philosophy that can be adopted to manage the system needs becomes crucial. For example, if the main objective is to satisfy the power demand, the steam supplied to the refinery must be manipulated in agreement with the specified setpoint. This means that when the generated power should be increased, the master control should increase the *char* load to the gasifier unit, until the temperature of the gas turbine combustion chamber achieves the maximum allowed. Then, the power production can be only increased by reducing the steam availability for external needs. Doing so, the steam turbine should be used in a specific range of operating conditions satisfying the gap between power production and external electrical load.

The aim of the present work is to study the dynamic behavior of such a IGCC process and to address the control design issue mentioned above. The gasification plant includes the synthesis gas production, the tail gas treatments, high, medium, low pressure steam production and the energy production in combined single-shaft steam and gas turbines. Simplified dynamic simulations reported in literature (Depew et al., 1997), seem to address a system with fast and instantaneous reaction so that it can be observed as a sequence of steady-state conditions rather than a time dependent evolution. In such a preliminary study significant inverse responses and nonlinear or delayed dynamic transients are not reported.

This result seems to suggest the use of a steady-state simulator (generally faster and more robust) instead of detailed dynamic one. However, the analysis of Depew et al. is conditioned by a transient analysis corresponding to very slow setpoint variations that allow considering the gasifier always at a steady-state regime. The only significant dynamics seems to be related to levels and pressures of some apparatuses that are mainly determined by the adopted control settings. This refers to local variables not affected by the main process dynamics. This last one is assumed to be mainly conditioned by negligible time constants (gas flow based). With such assumption, the need of a rigorous dynamic simulator becomes less important and the system could be represented by a sequence of steady-states. This philosophy leads to a master controller, based on a stationary simulation/optimizer tool that is adopted to define the new setpoints corresponding to feed variation and/or power requirements.

However, the typical disturbances that the master control should be able to face are fast (power demand changes related to peak needs), as well as the responses of the controlled variables (e.g. steam flow, gas pressure). Moreover, as we will show later, the analysis made by using a detailed dynamic model shows a nonlinear behavior with respect to char composition and load variations (power demand) that are very common and frequent disturbances in all plants. These observations are the reasons of a different approach followed by the present paper. Here, the master control philosophy is based on a dynamic prediction of the optimal system trajectory to reach new steady-state conditions. Each control action is determined by the solution of an optimization problem minimizing the errors between the control variables and the corresponding setpoints using, as degrees of freedom, all the manipulated variables. The prediction is based on a dynamic model. The control structure described is known as Model Predictive Control and has been implemented by the process industry from many years. For more details see, for example, Morari and Lee, 1999.

Despite the aforementioned nonlinearity of the process, a linear MPC performs quite satisfactory. This means that the MPC controller is based on a linear dynamic model which is derived from the detailed process simulator by ARX MIMO identification. Such an approach allows a significant reduction, in terms of time and costs, of the “step-tests” procedure usually performed on the real plant to generate the data set for system identification. Moreover, this approach can be adopted even if the plant is not available or is at the design stage, so that, it can be easily used to integrate process and control design.

Furthermore, when a detailed nonlinear dynamic model is available, the reliability of the derived control structure can be validated by extensive simulation and numerical analysis. In

particular, since a detailed first principle model consists of a system of differential algebraic equations (DAE), the control equations $y_i - y_{set,i} = 0$ can be added as constraint conditions and then solved directly by using the controlled variables y_i as state variables and the manipulated variables (input variables) as unknowns. The overall system equations (units behavior plus control equations) are solved (Gear and Petzold, 1984) together at each time step (direct approach). This is a model-based control algorithm where the desired system response (setpoint trajectory) is imposed and the values of the manipulated variables are numerically evaluated. Obviously, this will be possible only when the manipulated variables adopted have a faster dynamics than the corresponding imposed disturbances. Then the system is invertible, and if no hidden instabilities occur, the “ideal” solution for the control problem examined can be derived. Unfortunately, in most cases, the disturbances are faster than the corresponding actions of the manipulated variables and the system becomes not invertible unless we add a time delay on the desired response. In any case, the numerical solution requires a significant computation effort.

However, as shown in the results reported in this paper, the direct approach is still a good instrument for testing and validating the performance of the designed multivariable controller. We will show that the MPC approach performs satisfactorily and therefore that it can be implemented as a master controller for IGCC plant. The paper is organized as follows: first of all, we derive a detailed dynamic model of the whole plant; this includes the model of the gasification unit, the model of the Heat Recovery Steam Generator (HRSG) and Combined Cycle (CC) unit, plus some simplified models of the gas treatment section units. Then, we describe the master control problem and the MPC design. Finally, we show the effectiveness of the control scheme through simulation comparisons.

Process and Detailed Model

In this section the model equations and related hypotheses will be only sketched and summarized (further details are available in Rusconi et al. 1998, Rusconi et al. 1999, Rusconi 2000).

The analyzed plant is schematically reported in Fig.1. The first unit is the gasifier where the heavy hydrocarbon feed (*char*), steam and oxygen are fed concurrently. Through a partial combustion, the solid/liquid residual is converted in syngas rich in CO and H₂, which maintains a very high heating value. After a fast quenching stage, the syngas goes to the

sulfur removal unit and, in sequence, to the hydrogen removal which has the task to satisfy the refinery needs. Finally, the syngas is fed to the gas turbine. Then, the outlet hot gases are used to recover most of the heat content to generate high (HP), medium (MP), and low pressure (LP) steam (Heat Recovery and Steam Generation system). The HP steam, and partially MP, are used to generate electrical power in the steam turbine. LP steam, and the remaining MP, are used to cover the refinery consumption.

For the gasifier model we assume that its dynamic behavior can be reduced to a sequence of steady-state conditions, i.e., the apparatus is varying subject to external disturbances but instantaneously reaching a new steady-state. This hypothesis is supported by the evidence, as shown in the following, that the characteristic time of the reactors is generally around 10 seconds while the HRSG and the Combined Cycle have response time constants in the order of 20-40 minutes.

The reactor, sketched in Fig. 2, has been modeled as a heterogeneous plug flow reactor utilizing mass, thermal and momentum balances. The reactions in the kinetic scheme are those reported by Wen and Chaung (1979) and Govind and Shah (1984). An example of composition and temperature profiles versus the reactor length, as determined by the given model, is reported in Fig. 3 for a typical industrial size plant. Fig. 4 shows how the evolution is practically instantaneous and takes place in the first part of the reactor while in the remaining length and time (~ 8 s) the system stabilizes at the corresponding new steady-state conditions. Therefore, the simulation results reported here clearly show the very fast evolution of such a unit and they confirm the assumption of defining the syngas temperature and composition as a direct function of the inlet disturbances. For a more complete description of the system equations and the details on the assumptions we refer to the bibliography mentioned above.

The combined gas/steam cycles, in the most typical configuration, are constituted by the coupling between a gas turbine and a steam cycle where the steam is obtained through the heat recovered from the exhausted gases discharged by the gas turbine. The generated HP and MP steam are used totally and partially, respectively, in a steam turbine rotating on the same shaft as the gas turbine. The process flow diagram sketched in Fig. 5 is very simple and clearly shows the structure of the described section. The two heat vectors (steam and gas flows) are characterized by a sharp separation determined through the tube walls of the boilers. Therefore any mixing of the two flows is strictly avoided.

This solution can reach an efficiency value of 25-35% with a size ranging from 3 to 200 MW. For larger needs several groups can be mounted in parallel with a cogeneration of electrical power and steam up to 1000 MW.

To derive the dynamic model, the mass, energy and momentum balances are written under the hypothesis that the main time constants are related to the heat and mass capacities of the boiler drums and wall tubes. Gas exchangers are simulated by stationary energy balances. Gas and steam turbines are described through a mechanical energy balance around the shaft. Details on the mentioned models and assumptions are available in literature (Annaratone, 1985; Lozza, 1995; Rusconi, 2000).

In comparison with some previous works, the analysis made by using our model, which is simple but contains all the main dynamic components, clearly shows that the HRSG unit and the CCU have their own dynamics determined by the geometry and the operating conditions. In Fig. 6 some operating variables are reported. Here, slow or fast dynamics are shown but with a complete different shape and time evolution with respect to the forcing disturbances. In particular, Fig. 6.a shows some delay for the response of the inlet fresh feed water to the MP boiler drum with respect to a pulse disturbance on the MP steam demand. Moreover, in Fig. 6b the rotating speed shows an inverse response due to the air compressor mounted on the turbine shaft. In the beginning, there is a slight reduction of the combustion temperature for a quench effect of the incoming material flow. This effect is also highlighted by a reduction of the combustion air moved by the compressor, which can be related to the decrease of the shaft speed. However, even if governed by a greater time constant, the syngas increasing flowrate allows the combustion temperature to be increased, by therefore increasing the rotating speed. Furthermore, it is important to underline that the system also reveals the presence of some nonlinearity which can play a significant role in the effectiveness of the control algorithm. Fig. 7 shows the comparison between the behavior of the shaft rotating speed (without control loops) at two operating points significantly different in terms of syngas flowrate and power generation, but perturbed by the same disturbance.

In Fig. 7a the disturbance imposed is a variation of 6 MW on the external load, while in Fig. 7b the disturbance is an additional hydrogen flow to the refinery of about 800 kg/h. All the plant conditions corresponding to the two lines are exactly the same except the initial external electrical load, i.e., power production, that is different in the two cases: around 100 MW for the black line and 140 MW for the gray one, corresponding to the 60% or 90% of the maximum load allowed, that is a typical working range for such power production packages.

In both figures it can be clearly observed the presence of different gains and time constants related to the main controlled variable (rotating speed) which indicates a different dynamic behavior of the plant at different operating conditions.

Fig. 7b also reports again the presence of inverse response which can become significant through the magnitude of some disturbances, e.g., the hydrogen flow withdrawn for the refinery. This particular behavior can play an important role in the design of a reliable control algorithm which avoids undesired persistent oscillating behaviors.

The Master Control Problem

For IGCC plants there are at least two main philosophies that can be adopted for control purposes. When the main objective is to satisfy the power demand, the first approach consists of regulating the externally supplied steam in agreement with a specified setpoint. As a consequence, when an increase of the power generation should be accomplished, the master control must be able to increase the *char* load to the gasifier unit but, when the temperature of the gas turbine combustion chamber achieves the maximum allowed, the power production can be increased by reducing the steam availability for external needs. In such a way the steam turbine should be in condition to satisfy the gap between power production and external electrical load. A schematic representation of such control philosophy is reported in Fig. 8 and will be referred to as “load following” control scheme.

The global control strategy must take into account a large number of variables ranging from levels of boiler drums and steam pressures to oxygen/*char* and steam/*char* ratios. The main structure of the master control can be summarized as follows:

manipulated variables: *char* flowrate to gasifier, steam flowrate to turbine;

controlled variables: shaft rotating speed turbine regime, power production, external steam demand;

constraints: turbine combustion temperature, oxygen availability.

If composition measurements related to syngas are available, they can be used to predict the optimal value of the oxygen/*char* ratio and to optimize the “heat gas quality” of the outlet gasifier stream.

The second alternative control philosophy can be adopted when the main objective function is the external steam demand. The request of a greater external steam flowrate, for a given

power production, can be satisfied through an increase of the *char* load only if the turbine combustion temperature is below the maximum operating limit and if the oxygen ramp can be accomplished by the oxygen plant (this is actually a limit on the system velocity in achieving the new setpoint). If one of the previous conditions is not satisfied, the power setpoint will be decreased, so reducing the steam fed to the turbine, according to the increased external needs. Such a control strategy is referred to as “steam demand” to highlight that, in this case, the steam required by the refinery becomes crucial.

MPC design

As shown in the previous section, the system to be controlled consists, at least, of two manipulated variables (char flowrate to the gasifier and steam flowrate to turbine), three controlled variables (power production, shaft rotating speed and steam flowrate to the refinery) plus one constraint on the turbine combustion temperature. The power production has a zero static gain with possible unacceptable overshoots during the transient. This particular behavior is related to the mechanical balance around the shaft: it always reaches the imposed external load, i.e., the turbine follows the speed specifications imposed by the required electrical power production. Therefore, although the system is 3 x 2 (3 CVs, 2 MVs), the controller has enough degrees of freedom to control the process. The fast response requirements of the system suggest a possible application of a linear MPC to solve the master controller problem (Morari and Lee, 1999). For such a purpose, this work applies the MPC toolbox (Bemporad et al. 2000) to the detailed plant simulator in order to better understand the performances of such a control approach to a nonlinear complex process. In particular, the first principle model has been used in place of the real plant and the predictive controller is based on a linear model obtained through ARX MIMO identification.

Considering for simplicity the SISO (Single Input Single Output) case, the ARX model is described by the following linear difference equation (L. Ljung; 1997):

$$y(t) + a_1 \cdot y(t-1) + \dots + a_{na} \cdot y(t-na) = b_1 \cdot u(t-nk) + \dots + b_{nb} \cdot u(t-nk-nb+1) + e(t) \quad (1)$$

where na is equal to the number of poles, $nb-1$ the number of zeros and nk is the system time-delay (dead time).

In this work, a MIMO (Multi Input Multi Output) ARX structure is adopted. For multi-input multi-output systems the coefficients a_i become a $n_y \times n_y$ matrix while the coefficients b_i a $n_y \times n_u$ matrix, where n_y is the number of the output variables and n_u the number of the inputs. The numbers na , nb and nk become the order matrices, with $n_y \times n_y$ and $n_y \times n_u$ elements respectively; na is a matrix whose i-j entry is the order of the polynomial (in the delay operator) that relates the j-th output to the i-th output; nb is a matrix whose i-j entry is the order of the polynomial that relates the j-th input to the i-th output; nk is a matrix whose i-j entry is the delay from the j-th input to the i-th output.

Formally a multivariable ARX model is given by:

$$A(q) \cdot y(t) = B(q) \cdot u(t) + e(t) \quad (2)$$

where $e(t)$ is a noise vector taking into account external disturbances and unmodeled dynamics. In the IGCC plant problem a structure with four outputs (three controlled variables plus one output subject to constraints) and four inputs (two manipulated variables plus two measured disturbances) has been adopted to approximate the system behavior via the linear model (2).

The role of the variables involved in the IGCC control problem is summarized in Table 1. It should be noted that, in the control configuration, the value of the measured disturbance, related to the electrical load, coincides with the generated power setpoint. In other words, the external electrical load is a feedforward variable which defines the setpoint of the power production but the plant has a self balance around the shaft such that power production and external load finally become always equal. This implies that the power production has a zero static gain with respect to the main possible disturbances but it can still have excessive transient overshoots. Therefore, matching the external load value, the shaft rotating speed runs away from its setpoint giving rise to a bad quality of the electrical energy production ($\cos\phi$ variation). As a consequence, in the identification procedure, the external electrical load is treated as an input like the hydrogen flowrate to the refinery and the manipulated variables.

The order matrices chosen for identification are:

$$na = \begin{bmatrix} 2 & 2 & 2 & 2 \\ 2 & 2 & 2 & 2 \\ 2 & 2 & 2 & 2 \\ 2 & 2 & 2 & 2 \end{bmatrix}, \quad nb = \begin{bmatrix} 2 & 1 & 2 & 1 \\ 2 & 1 & 2 & 1 \\ 1 & 1 & 2 & 1 \\ 2 & 1 & 2 & 1 \end{bmatrix}, \quad nk = \begin{bmatrix} 1 & 1 & 1 & 1 \\ 1 & 1 & 1 & 1 \\ 1 & 1 & 1 & 1 \\ 1 & 1 & 1 & 1 \end{bmatrix}.$$

In the ARX identification each row is identified independently from the others so it is quite simple to modify the orders and the delays for each output and verify the proper choice of the structure. The model accuracy achieved is satisfactory, not only around the operating conditions where the step tests have been performed, but also far away from it. Nevertheless, it must be underlined that the identification of the best model for process analysis purposes is not the aim of this work, what we need is only a proper model for the MPC algorithm. The next step is to verify if a linear MPC can be effective and of real value to cover all the control objectives, despite the fact that the plant behavior is highly nonlinear. Note that a detailed first principle model cannot be used in a nonlinear MPC scheme because the complexity of the resulting nonlinear optimization problem would be computationally infeasible.

Usually the minimum sampling time is dictated by the control computer. Here, the sampling time has been fixed on the basis of the following rule of thumb (Ljung, 1996):

$$\text{sampling time} = \min \{0.03 \text{ settling time}, 0.3 \text{ deadtime}\}.$$

Referring to several open-loop simulations corresponding to alternative disturbances, the results indicate a sampling interval ranging between 40-60 seconds, which is feasible for implementing the linear MPC controller on the control hardware available at the IGCC plant. In order to have a suitable set of data for identification, a long simulation has been carried out starting from the steady state of a typical operating point and giving first a series of positive and negative steps at each variable separately and then combining them together. The identified model was validated on a different set of data (validation data), as shown in Fig. 9, where the output variables for the identified ARX model. The responses are referred to a series of step disturbances and are represented in terms of delta with respect to the initial value.

Once a good the linear model of the IGCC process is obtained we use it within the Model Predictive Control SIMULINK Library (Bemporad et al., 2000). The MPC block is based on the prediction model schematically reported in Fig. 10. This can be conveniently described by the state-space form:

$$\begin{cases} x(k+1) = A \cdot x(k) + B_u \cdot u(k) + B_v \cdot v(k) + B_d \cdot d(k) \\ y(k) = C \cdot x(k) + D_v \cdot v(k) + D_d \cdot d(k), \end{cases} \quad (3)$$

where $x(k)$ represents the state of the system, $u(k)$ are the manipulated variables (MV), $v(k)$ is a vector of measured disturbances (MD), $d(k)$ are unmeasured disturbances (UD) and $y(k)$ is the output vector, which is composed of measured outputs (MY) and unmeasured outputs (UY). Note that no direct feedthrough of MVs on the output vector is allowed.

The identified ARX model (2) is automatically converted to the form (3) by the aforementioned MPC library. The MPC controller selects the input $u(k)$ by solving the optimization problem:

$$\left\{ \begin{array}{l} \min_{\Delta u(k|k), \dots, \Delta u(m+1+k|k)} \sum_{i=0}^{p-1} \left\{ \|\omega_i^u [u(k+i|k) - u_{\text{target}}(k)]\|^2 + \|\omega_i^{\Delta u} \Delta u(k+i|k)\|^2 + \|\omega_{i+1}^y [y(k+i+1|k) - r(k+i+1)]\|^2 + \rho_\varepsilon \varepsilon^2 \right\} \\ \text{subj. to } \begin{cases} u_i^{\min} \leq u(k+i|k) \leq u_i^{\max} \\ \Delta u_i^{\min} \leq \Delta u(k+i|k) \leq \Delta u_i^{\max} \\ -\varepsilon + y_i^{\min} \leq y(k+i+1|k) \leq y_i^{\max} + \varepsilon \\ \Delta u(k+j|k) = 0, \quad j = m, \dots, p \\ \varepsilon \geq 0 \end{cases} \end{array} \right. \quad (4)$$

with respect to a sequence of future input increments $\{\Delta u(k|k), \dots, \Delta u(m-1+k|k)\}$ and the slack variable ε , which represents the violation of the output constraints. In Eq. (4) $(k+i|k)$ denotes the value predicted for time $k+i$ based on the information available at time k ; $r(k)$ is the current sample of the output reference. While only the measured outputs are connected to the simulation block (see Fig. 11), $r(k)$ is a reference for all outputs (measured and unmeasured).

Note that inputs and input variations are treated as *hard constraints*, while output constraints are considered as *soft* which means that they can be violated in a $\pm \varepsilon$ range, which is penalized by the term $\rho_\varepsilon \varepsilon^2$ in the cost function. This prevents the MPC controller to get stuck because of infeasibility of the optimization problem. $u_{\text{target}}(k)$ is a setpoint for the input vector, which in our application is set to zero. Weights on inputs variations and lower/upper bounds were imposed. Only $\Delta u(k|k)$ is used to compute $u(k)$, the remaining samples are discarded and a new optimization problem based on new measurements is solved at time $k+1$. As the

true states of the system are not available, state estimates are obtained from the measured output using a Kalman filter. The algorithm uses different solving procedures depending on the presence of constraints; in the case of a constrained problem, as the current one, a Quadratic Programming (QP) solver is adopted.

The first principle model (implemented in FORTRAN) of the open-loop system has been interfaced with SIMULINK by using the Application Program Interface tools, by transforming the FORTRAN code to a discrete-time MEX S-Function, which allows the detailed dynamic simulator and the MPC tool to be used within the SIMULINK environment. It should be noted that the system function containing the model for SIMULINK must be discrete-time as the model describing the process contains differential algebraic equation, and therefore it cannot be directly integrated by SIMULINK.

The derived SIMULINK scheme is reported in Fig. 11. The IGCC plant S-function block contains the FORTRAN detailed model while the MPC controller block contains the controller algorithm that uses the identified linear model. All the parameters, such as the weights, limits input targets, control and prediction horizon, can be easily changed through a dialog mask.

The MPC algorithm handles the turbine temperature as a controlled variable with zero weight. Such an assumption implies that only a potential violation of its limits, the upper one in particular, can generate a significant control action. As mentioned above, the electrical load changes are at the same time measured disturbances and setpoint changes, as shown by the connecting lines in the Fig. 11. The reported scheme also contains the inlet char composition disturbances that are unmeasured and not modeled.

Validation and Performance Checks

The MPC controller in closed-loop with the detailed FORTRAN simulator was extensively tested and the control performance compared with the one achievable by conventional controllers and ideal solutions.

After some tuning trials, the optimization of the system response in terms of QP complexity and settling time brings to a prediction horizon of 18 sampling instants and to a control horizon (free moves) of 3.

A summary of the numerical value for the control settings is listed in Table 2.

The first set of plots reported in Fig. 12 refers to a typical load change. The external electrical grid requires an increase of the power production of 20 MW (from 134 to 154 MW) which will be imposed as a feedforward variable disturbance (or measured disturbance, see Table 1) through a ramp variation in 10 minutes. It can be observed that this can be achieved by moving the char feed and steam to the turbine while the main controlled variables (steam to refinery and shaft speed) are maintained very close to their setpoint.

The second set of data reported in Fig. 13 is similar but refers to a larger change in the power production, from 134 MW to 161 MW. Therefore, the turbine combustion temperature reaches its upper limit and no more char is fed to the gasifier. Conversely, the controller tries to match the power requirement by violating the controlled variable “steam to refinery”, so allowing an increase of the power production by means of the steam to the turbine.

Such a "load following" philosophy is simply realized by choosing different weights for the "steam to refinery" with respect to the other controlled variables. In particular, a smaller value allows the steam request to be penalized with respect to the power generation.

With the aim of checking the performance of the MPC controller versus a more conventional solution, Fig. 14 shows the comparison between PI control action and MPC when the power setpoint variation is imposed. The reference PI control configuration is listed in Table 3. The corresponding controller setting has been determined on the basis of an ISE method. The reported results show that the MPC solution is less oscillating, which generally means better quality production ($\cos\phi$ related to the shaft speed), savings (peak value of generated power), and a system working more properly close to its constraints.

Finally, in order to obtain a performance evaluation of the designed linear controller, the “direct” solution to the control problem was calculated. In mathematical terms, the ideal control problem can be represented as follows:

$$\begin{cases} \underline{y}' = f(x, \underline{y}, \underline{y}') \\ g(x, \underline{y}, \underline{y}') = 0 \end{cases}$$

$$y_n - y_{set,n} = 0, \quad n = 1, \dots, n_c,$$

where n_c is the number of controlled variables.

The resulting DAE system represents the detailed model of the process plus the ideal control equations where the controlled variables are imposed always equal to the setpoint along time. The degrees of freedom corresponding to those last equations are the manipulated variables whose variations are determined simultaneously to match all setpoints step by step. The main

question related to this approach is that the dynamic solution of the DAE system is strictly related to the dynamic of the considered disturbances.

In other words, similarly to a feedforward control design, if the dynamics effect of the forcing disturbances on the controlled variables is faster than the corresponding manipulated variables the solution does not exist.

However, when the solution is available it represents the ideal way to match the desired setpoints and it can be of real value to judge the effectiveness of the designed MPC controller. Fig. 15 shows the comparison between the linear MPC and the corresponding “ideal” solution with respect to a classical setpoint variation of the generated power demand. Observing both the manipulated variables (steam to turbine and char) and the controlled variables, it is clear that the linear MPC solution is rather closed to the “ideal” solution. A more detailed MPC tuning can even improve the control performance. However, from the results reported here, it must be underlined that the maximum rotating speed error is around 0.15 rpm, which is in the range of the noise affecting such measurements, while the maximum MP steam flowrate error is less than 1%, which is also a typical flowrate measurement error.

Conclusions

The availability of a detailed dynamic model of an IGCC plant allows the design of a linear Model Predictive Controller. Although the system shows the presence of some nonlinearity and the control tool requires a fast response to power demand changes, the designed linear MPC turns out to be robust, reliable with respect to alternative process conditions, and of real value for practical purposes.

An easy and friendly MATLAB/SIMULINK environment allows the use of the System Identification and MPC toolboxes together with a complex FORTRAN nonlinear simulator.

Such an approach can be generally applied whenever a simulator is available, reducing the need for extensive tests (identification and tuning) during the commissioning phase of the MPC project.

References

Annaratone D., “Generatori di Vapore”, CLUP, Milano, (1985). In Italian.

Bemporad A., M. Morari, N. L. Ricker, ‘The MPC Simulink Library’, The Math Works Inc. 2000. <http://control.ethz.ch/~bemporad/toolbox>

Depew C., A. Martinez, G. Collodi, R. Meloni, “Dynamic Simulation for IGCC Plant Process and Control Design”, AspenWorld 1997, Boston (USA), Ottobre 12-16, 1997.

Gear C., Petzold L., “ODE Methods for the Solution of Differential/Algebraic Systems”, Siam. J. Numer. Anal. 21, n. 4, Aug. (1984).

Govind R., J. Shah, ‘Modeling and Simulation of an Entrained Flow Coal Gasifier’, AICHE Journal, Vol. 30, No. 1, January 1984.

Ljung L., "System Identification Toolbox for Use with Matlab", Using Matlab (version 6.0), The Math Works Inc.

Ljung L., "System Identification", The Control Handbook, 1996 CRC Press, Inc.

Lozza G., “*Turbine a Gas e Cicli Combinati*”, ed. Progetto Leonardo, Bologna, (1995). In Italian.

Morari M., J. H. Lee “Model Predictive Control: Past, Present and Future”, Comp. Chem. Eng., 23, 4, 667-682 (1999).

Parkinson G., K. Fouhy, “Gasification: New Life for an Old Technology”, Chem. Eng., 37-43 (March, 1996).

Rusconi F., M. Rovaglio, D. Manca, "Simulazione Dinamica e Controllo dei Processi di Gassificazione con Relativo Ciclo Combinato per la Cogenerazione di Energia" (GRICU Proceedings, Ferrara 1998). In Italian.

Rusconi F., M. Rovaglio, D. Manca, "Direct Model Predictive Control of Integrated Gasification"; IcheapP4-99 Proceedings (Firenze, 1999).

Rusconi F., “Controllo Predittivo per Processi di Gassificazione con Ciclo Combinato”, PhD Thesis, Politecnico di Milano, 2000. In Italian.

Wen C. Y., T. Z. Chaung, “Entrainment Coal Gasification Modeling”, Ind. Eng. Chem. Des. Dev., Vol. 18, No. 4, 1979.

List of figures

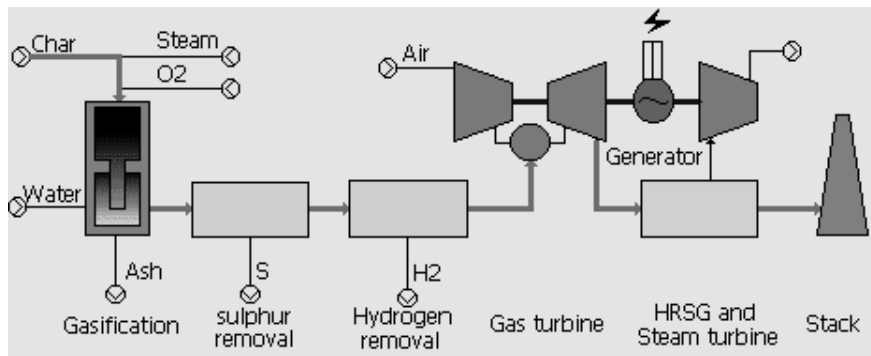


Fig. 1: Schematic Process Flow Diagram of an IGCC plant

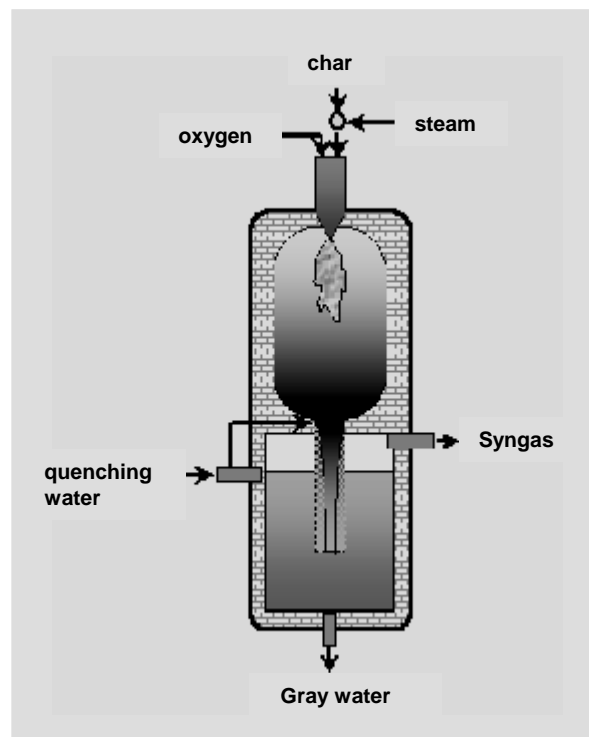


Fig. 2: The gasification reactor

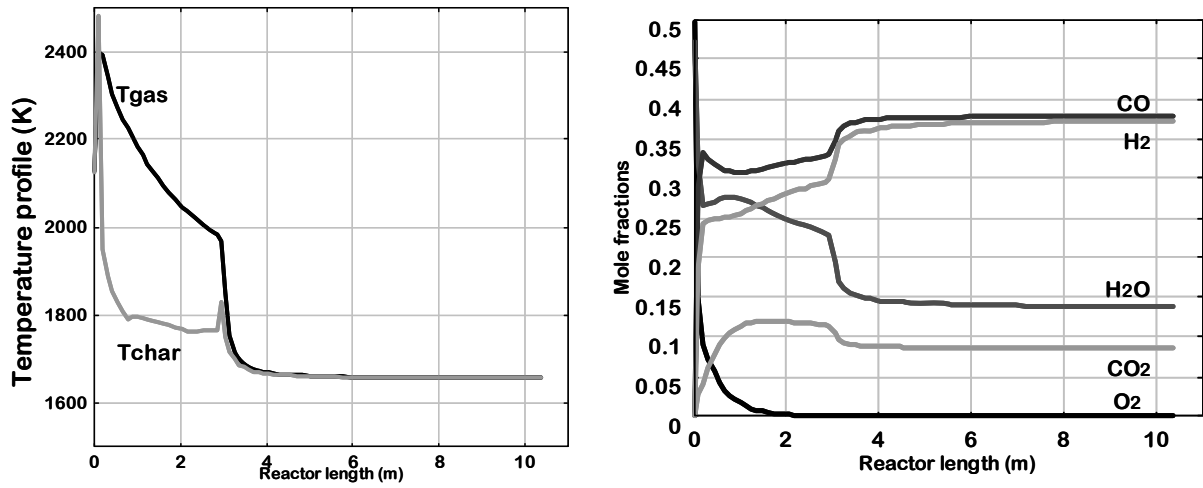


Fig. 3: Temperature (K) and composition profiles versus gasifier residence time (s)

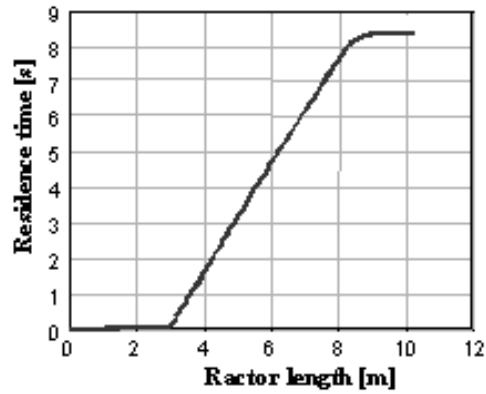


Fig. 4: Residence time (s) versus reactor length

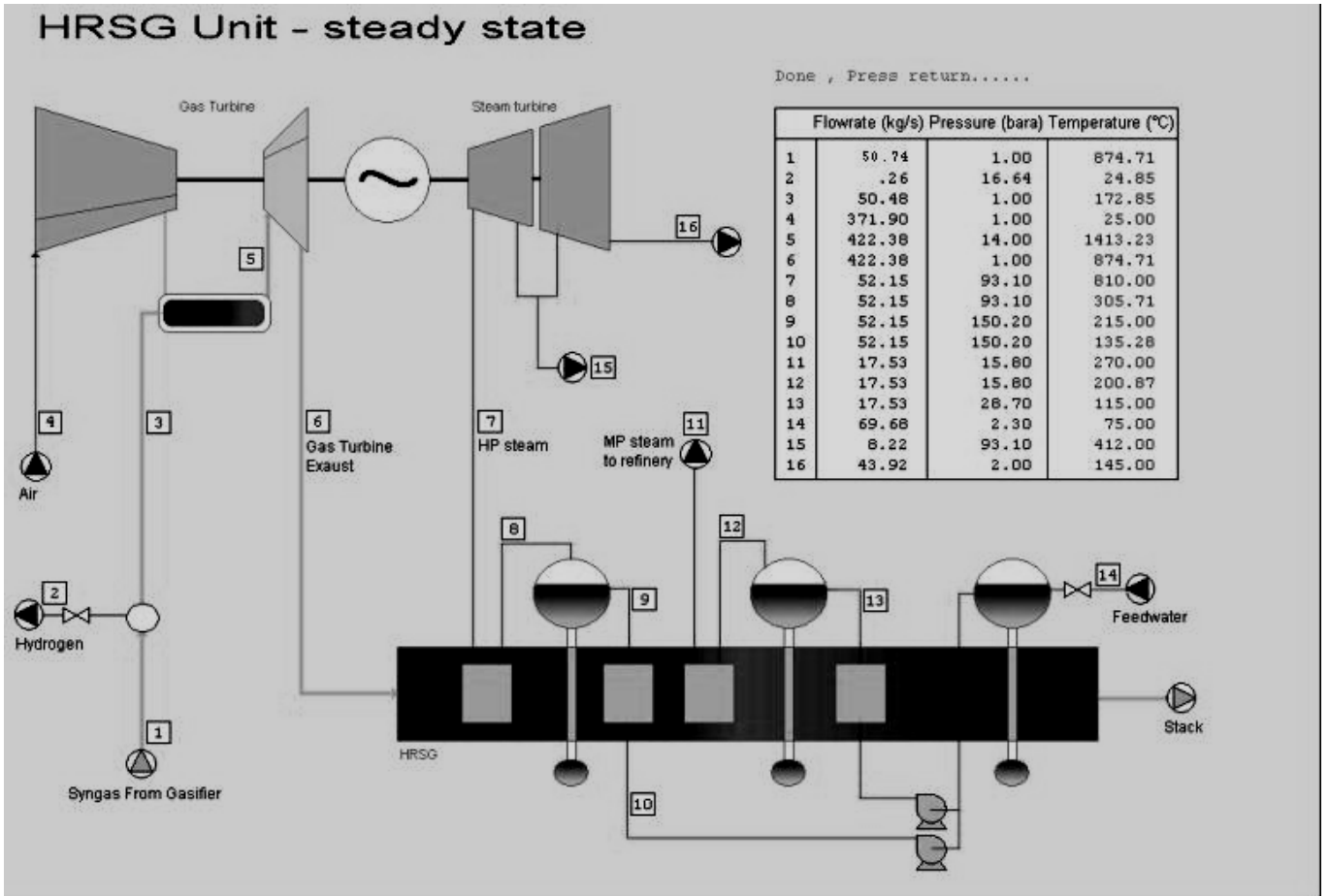


Fig. 5: Process flow diagram for the CCU and the HRSG sections

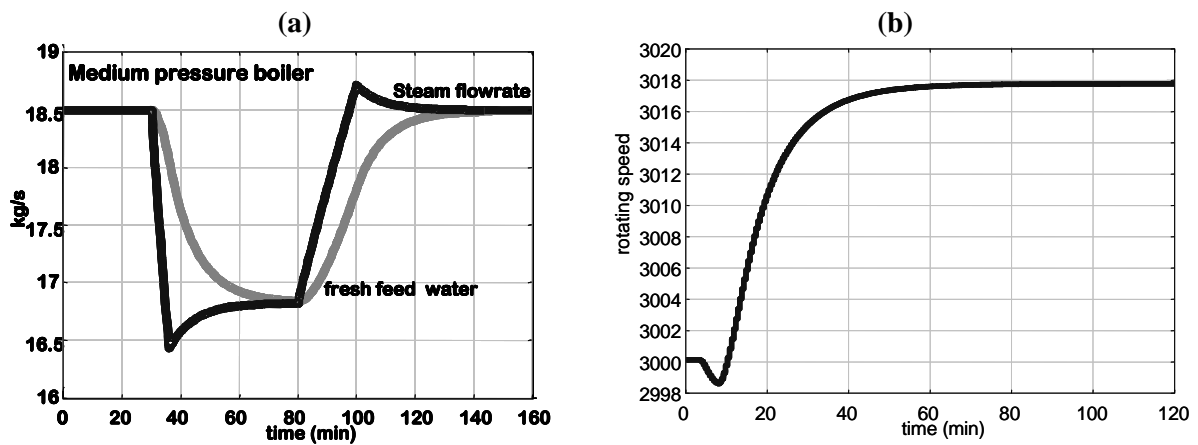


Fig. 6: Dynamic behavior of CCU and HRSG systems:

- (a) delay of the inlet water flowrate to the MP boiler drum with respect to a steam demand disturbance;
- (b) inverse response of the turbine shaft with respect to an increase of the syngas flowrate

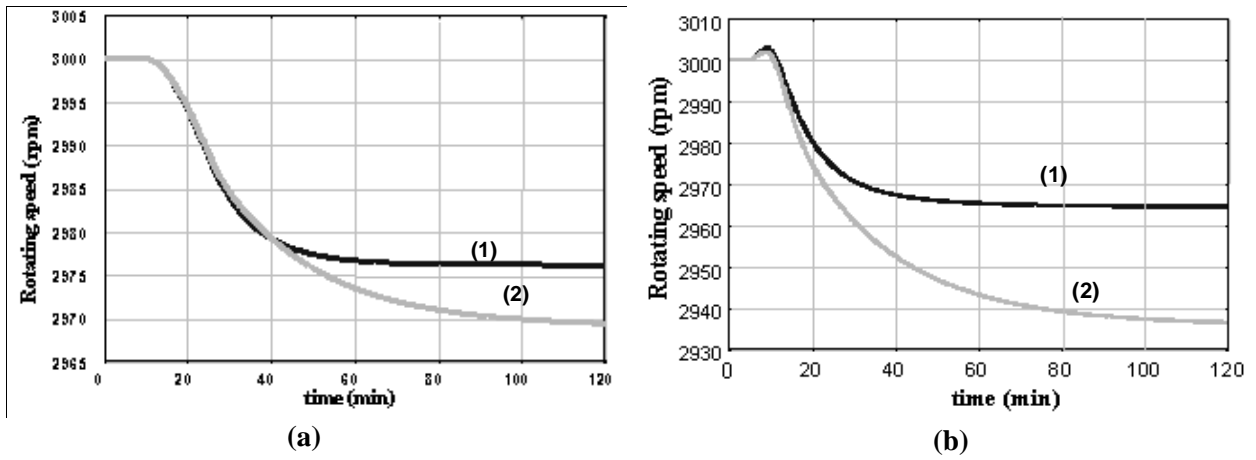


Fig. 7: Shaft rotating speed in different operating conditions (1) 100 MW (2) 140 MW and with respect to different disturbances:
 (a) 6 MW for the external electrical load
 (b) 800 kg/h of H₂ withdrawal for the refinery

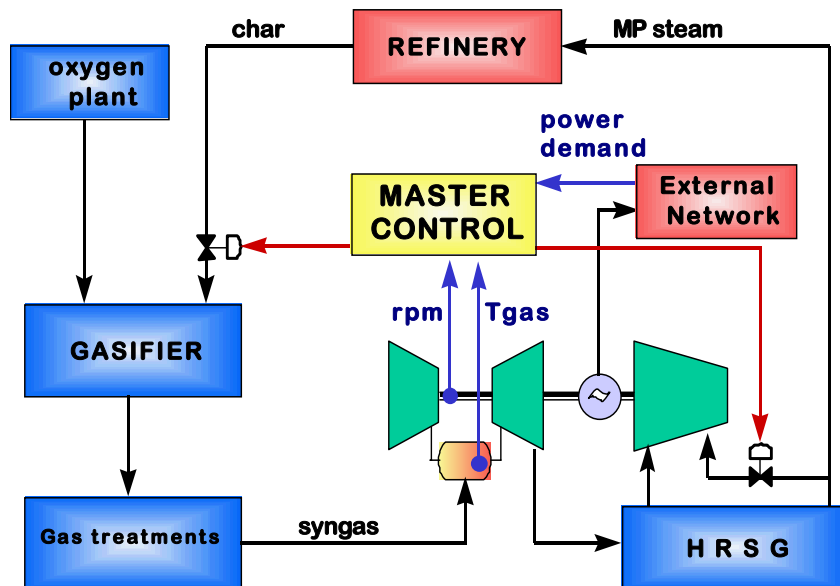


Fig. 8: "Load following" control scheme

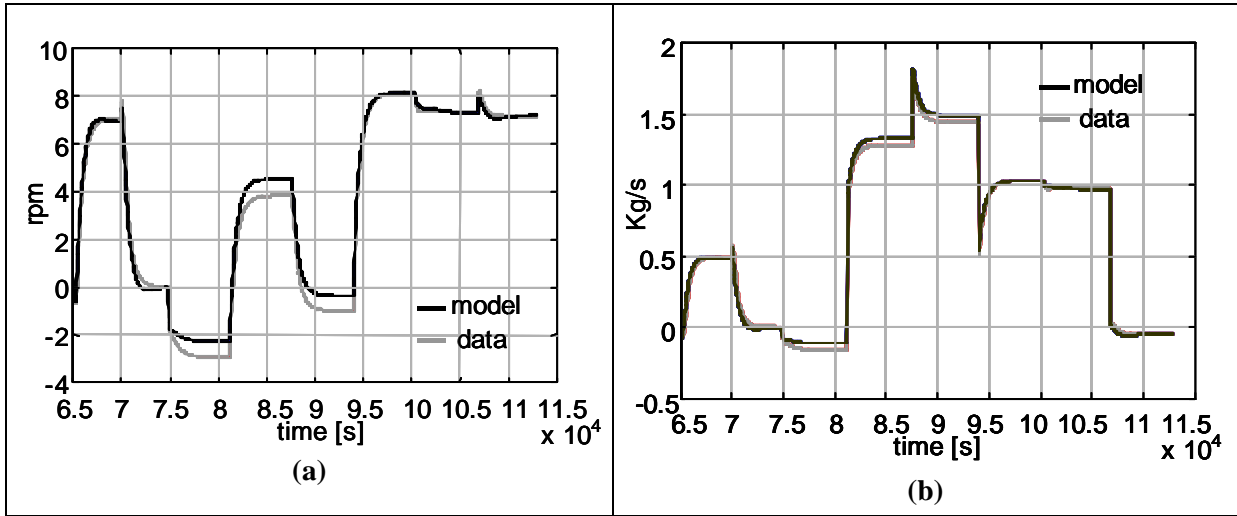


Fig. 9: Validation of the output variables for the identified ARX model:
 (a) – shaft rotating speed (rpm)
 (b) – steam flowrate to refinery (kg/s)

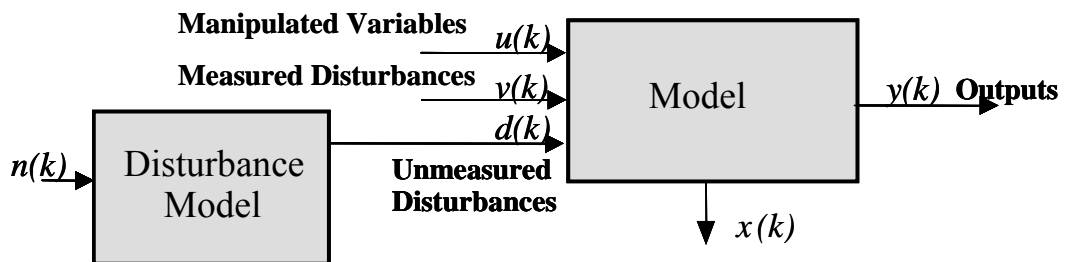


Fig. 10: Prediction model used by the MPC SIMULINK library

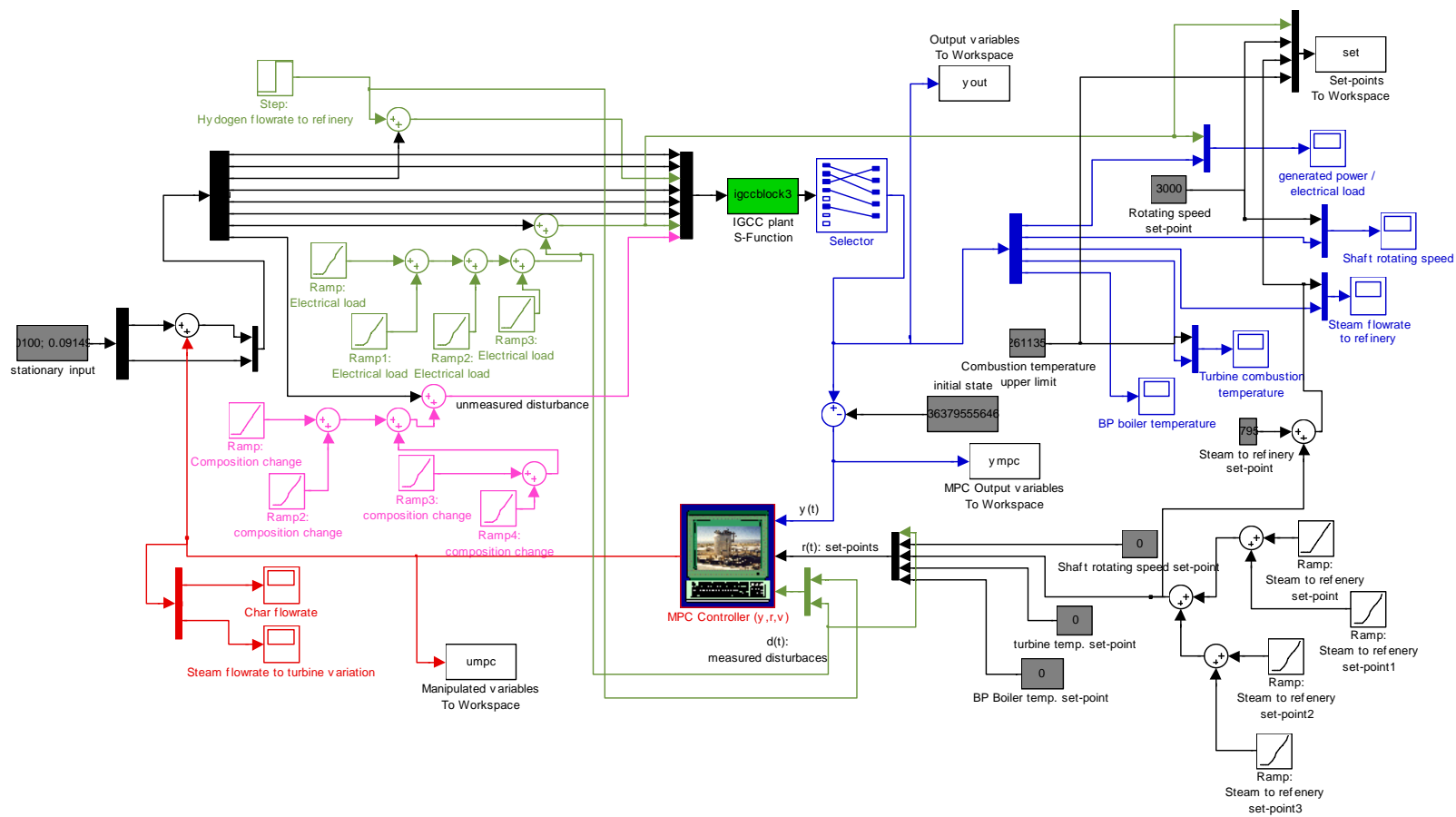


Fig. 11: SIMULINK model

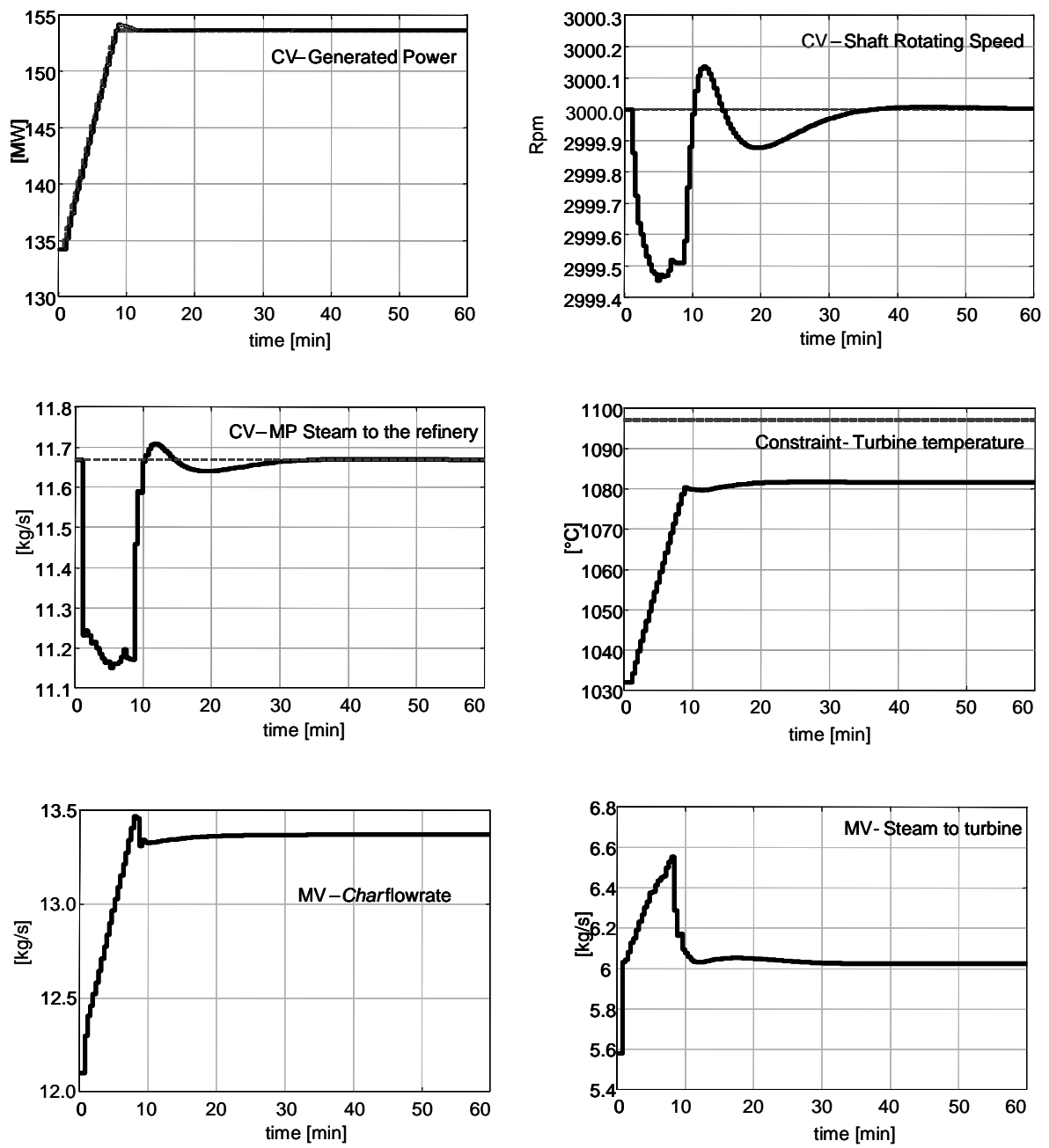


Fig. 12 – Simulation of a 20 MW load change: controlled and manipulated variables

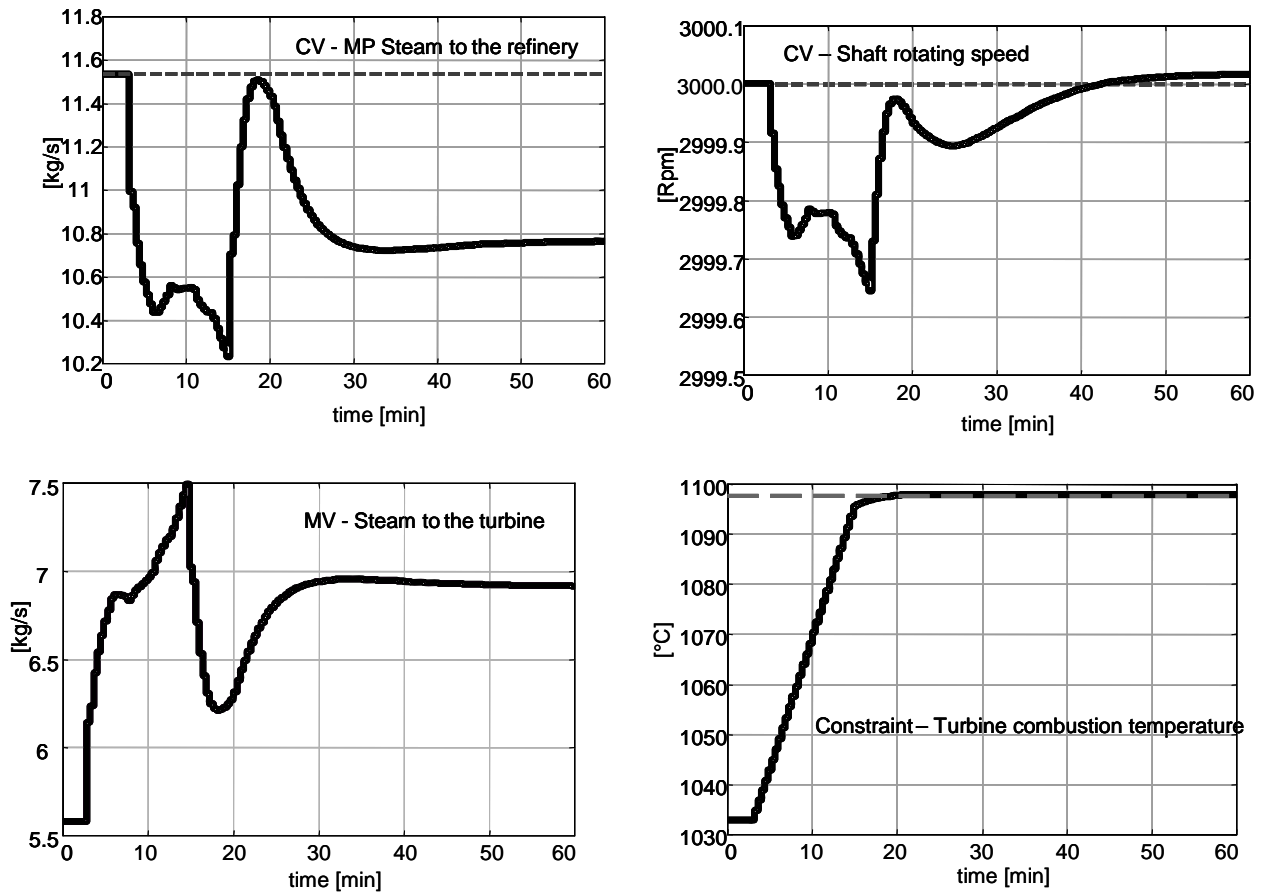


Fig. 13 – Simulation of a 27 MW load change: controlled and manipulated variables

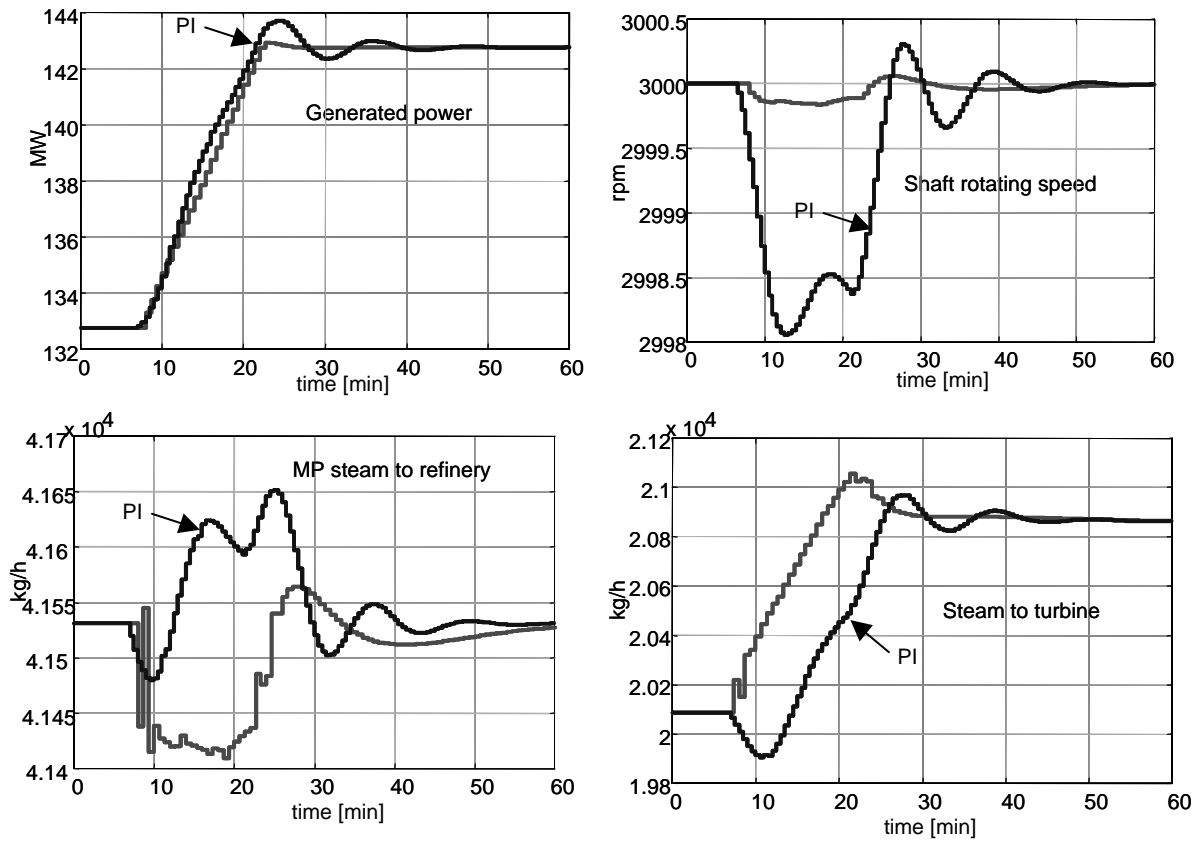


Fig. 14 – Comparison between linear MPC and a PI controller: load change simulation

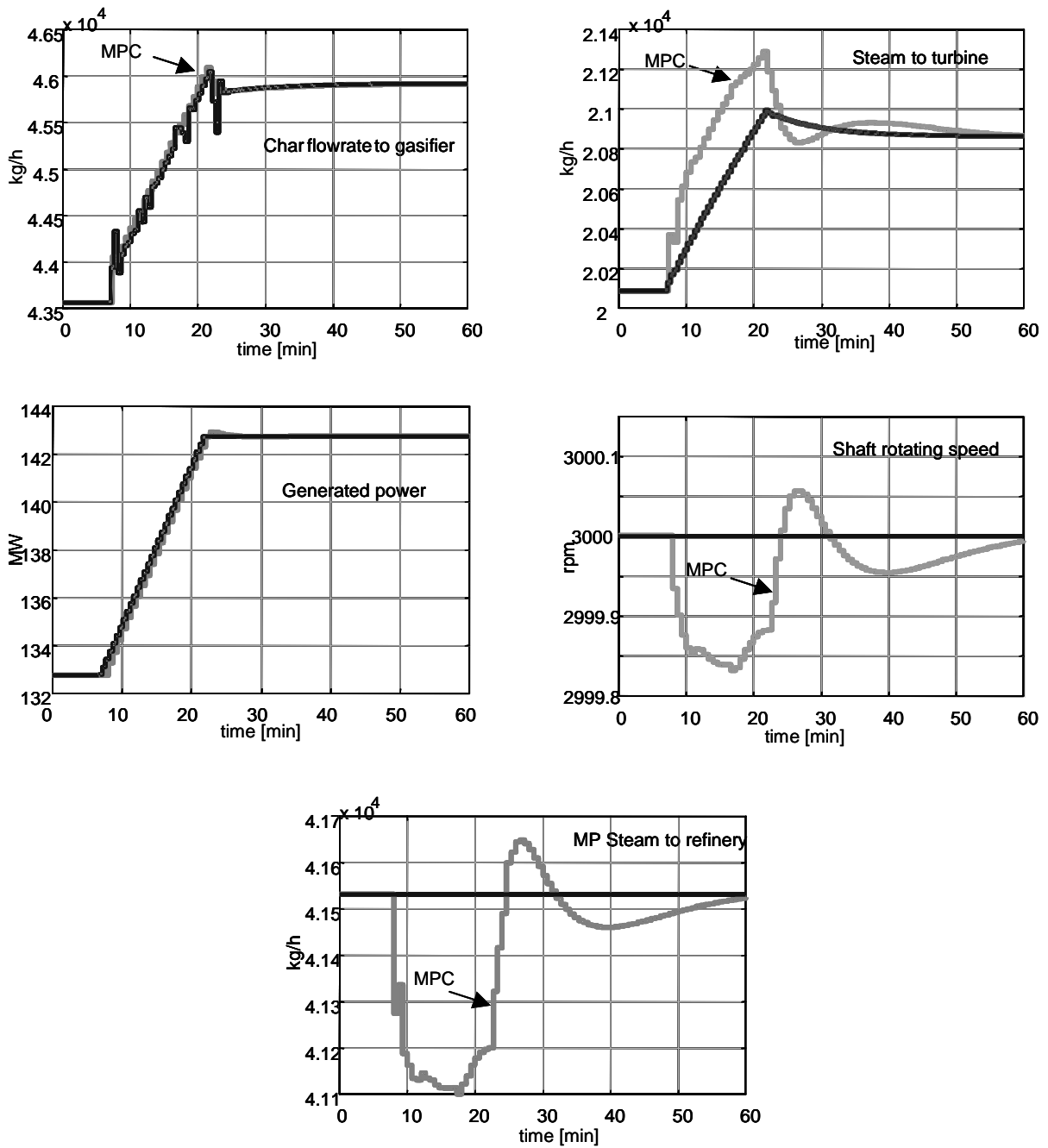


Fig. 15: Comparison between linear MPC and the ideal solution: load change simulation

List of tables

Controlled variables	Constraints	Manipulated Variables	Measured Disturbances
Generated Power	Turbine temperature	Char Inlet Flowrate	H ₂ Flowrate to Refinery
Shaft Rotating Speed		Steam Flowrate to Turbine	External Electrical Load
Steam Flowrate to Refinery			

Table 1: IGCC control problem scheme

Sampling time	40 seconds		
Prediction horizon	18 (number of sampling intervals)		
Control horizon (moves)	3 (number of sampling intervals)		
Manipulated variables setpoints (target)	zero		
Controlled variables weights	Power	Shaft rotating speed	Steam flowrate to refinery
	1	1	0.5
Manipulated variables weights	Char flowrate		MP steam flowrate to refinery
	0.2		0.1

Table 2: MPC controller parameters

Controlled Variables	Manipulated Variables	Controller Type
Shaft rotating speed	Syngas Flowrate	PI
Syngas Manifold Pressure	Char Flowrate	PI
MP Steam flowrate to refinery	Valve of MP Steam to refinery	PI

Table 3: Basic PI control configuration